

# CONDUCTION BAND-VALENCE BAND THEORY OF TL AND OSL: EMPHASIS ON DELOCALIZED TRANSITIONS AND EXPLANATION ON SOME UNUSUAL EFFECTS

Reuven Chen \*

School of Physics and Astronomy, Tel Aviv University, Tel Aviv 69978, Israel

\*Corresponding author: chenr@tau.ac.il

Received 19 October 2020; revised 19 October 2020; editorial decision 26 November 2020; accepted 26 November 2020

We discuss some unusual thermoluminescence (TL) and optically stimulated luminescence effects. We focus on luminescence due to transitions of electrons or holes through the conduction or valence band, respectively. We deal with non-linear dose dependence and non-monotonic dose dependence and also dose-rate effects sometimes reported. Also, is discussed the sensitisation of a sample due to the combined effect of irradiation and annealing, occurring in quartz samples and other materials. Another effect presented is the occurrence of anomalously high activation energies and frequency factors and its possible theoretical interpretation. Also, are considered the effects of anomalous fading and anomalous stability. Yet another phenomenon is concentration quenching. Here, the intensity of emitted TL depends non-monotonically on the concentration of the impurity responsible for the emission. The explanations given to these phenomena are based on the numerical solutions of the relevant sets of differential equations as well as approximate analytical treatment.

## INTRODUCTION

In this chapter, thermoluminescence (TL) and optically stimulated luminescence (OSL) effects associated with charge trapping and transitions through the conduction and valence bands during excitation and thermal/optical stimulation are considered. In some cases, the theoretical explanation is associated with uniform excitation of the sample in hand, such as is approximately the case with  $\beta$  rays, and certain wavelengths of ultraviolet (UV) or X-ray excitation and rather thin samples. Some unusual effects will be discussed in detail along with their possible explanations.

The fundamental model of TL and OSL has to do with the energy band model of insulators. One considers the last filled band, which is called the valence band, the first allowed but empty band above it, which is called the conduction band, and the forbidden band in between. In a hypothetical pure crystal, there are no allowed levels in the forbidden gap. However, practically all crystals have imperfections, namely impurities and defects, which produce allowed electron- and hole-traps. The very basic model (Randall and Wilkins<sup>(1)</sup>) assumes for simplicity the occurrence of only one kind of electron trap, residing rather close to the conduction band, and one kind of hole trap located rather far from the valence band. Due to its role in the read-out stage (heating in TL or light exposure in OSL), the hole trap is usually referred to as a recombination centre, as explained below. A schematic diagram is shown in Figure 1. When the sample is irradiated, it is assumed that electrons are

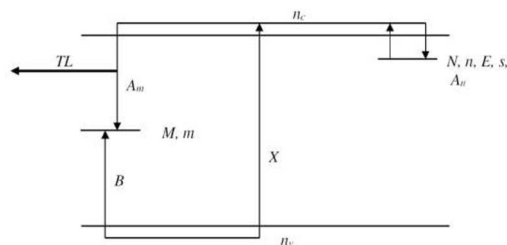


Figure 1: One trap and one recombination centre energy level scheme.

being raised from the valence band into the conduction band. The electron in the conduction band may move in the crystal and be trapped in the electron trap. The created hole may move in the valence band until it is trapped in the hole centre.

It is worth mentioning that the inverse model is just as likely to occur. Here, we assume that the hole traps are rather close to the valence band so that they may be released thermally into the valence band during the read-out stage. The electron traps are rather far from the conduction band and therefore their role is passive. If holes released from the hole traps, which are in the valence band, they may encounter a trapped electron and recombine emitting a photon. Under these circumstances, the electron trapping state is referred to as an electron recombination centre. For the sake of simplicity, we will usually talk about the former, namely, systems with electron traps and hole

recombination centres, but we will keep in mind that the inverse model is also viable.

At the end of the irradiation stage, if there are electrons left in the conduction band, they are expected to get either trapped or recombine with holes in centres during the 'relaxation time' until the number of electrons in the conduction band is practically zero. If there are holes left in the valence band, they will be trapped in the hole centres during the relaxation time.

The next stage is the read-out, which in TL is performed by heating the sample, usually at a constant rate, and measuring the emitted light in the course of the heating. During the heating, electrons are thermally raised from the traps into the conduction band from which they may either retrap or perform recombination with a hole in a centre. Figure 1 depicts schematically the basic one-trap-one-recombination-centre (OTOR) model, also termed 'general one trap (GOT)'. The relevant magnitudes shown are  $N$  ( $\text{cm}^{-3}$ ) the concentration of relevant traps,  $n$  ( $\text{cm}^{-3}$ ) the instantaneous concentration of trapped electrons,  $M$  ( $\text{cm}^{-3}$ ) concentration of recombination centres,  $m$  ( $\text{cm}^{-3}$ ), the instantaneous concentration of holes in traps,  $E$  (eV) the activation energy for the release of electrons into the conduction band,  $s$  ( $\text{s}^{-1}$ ) the pre-exponential frequency factor,  $n_c$  ( $\text{cm}^{-3}$ ) and  $n_v$  ( $\text{cm}^{-3}$ ) the instantaneous concentrations of free electrons and holes, respectively.  $A_m$  ( $\text{cm}^3 \text{s}^{-1}$ ) and  $A_n$  ( $\text{cm}^3 \text{s}^{-1}$ ) are the recombination and retrapping probability coefficients of free holes, respectively.  $B$  ( $\text{cm}^3 \text{s}^{-1}$ ) is the trapping probability coefficient of free holes into the centres and  $X$  ( $\text{cm}^{-3} \text{s}^{-1}$ ) is the rate of production of electron-hole pairs by the irradiation, which is proportional to the dose rate.

Let us concentrate first on the process taking place during heating. The set of kinetic equations governing the process as given by Halperin and Braner<sup>(2)</sup> is

$$\frac{dn}{dt} = A_n(N - n)n_c - sn \exp(-E/kT), \quad (1)$$

$$I(T) = -\frac{dm}{dt} = A_m m n_c, \quad (2)$$

$$\frac{dm}{dt} = \frac{dn}{dt} + \frac{dn_c}{dt}, \quad (3)$$

where  $k$  ( $\text{eV} \cdot \text{K}^{-1}$ ) is Boltzmann's constant and  $I(T)$  the intensity of emitted TL. In order to be able to simulate a conventional TL curve, one has to use some heating function, which in many cases is chosen to be linear with time, namely, a constant heating rate is used

$$T = T_0 + \beta t, \quad (4)$$

where  $T_0$  (K) and  $T$  (K) are the initial and running temperatures and  $\beta$  (K/s) is the constant heating rate. It should be mentioned that here, we associate the emitted intensity,  $I(T)$  with the rate of decrease of the concentration of holes in centres. As appearing here, the units of  $I(T)$  are  $\text{cm}^{-3} \text{s}^{-1}$  and in order to have it in light-intensity units, a dimensional constant should be added, which here has arbitrarily been set to unity.

The set of Equations (1-4) by Halperin and Braner<sup>(2)</sup> enable the general treatment of a single TL peak associated with a single trap and a single kind of recombination centre, but these equations were preceded by simpler equations by Randall and Wilkins<sup>(1)</sup> and by Garlick and Gibson.<sup>(3)</sup> Randall and Wilkins<sup>(1)</sup> assumed that recombination is very fast as compared with retrapping and ended up with a first-order equation governing TL, whereas Garlick and Gibson<sup>(3)</sup> assumed that the recombination and retrapping probabilities are equal and showed that second-order kinetics may govern the process. Let us see how these two situations emerge by making simplifying assumptions to the mentioned set of Equations (1-3).

Halperin and Braner<sup>(1)</sup> made the simplifying hypothesis later termed 'quasi-equilibrium' assumption stating that the instantaneous concentration of free electrons is significantly smaller than that of trapped electrons and holes and the rate of change of free electrons is significantly smaller than that of trapped electrons and holes,

$$\left| \frac{dn_c}{dt} \right| \ll \left| \frac{dn}{dt} \right|, \left| \frac{dm}{dt} \right|; \quad n_c \ll n, m. \quad (5)$$

Note that within the model discussed here, due to Equation (5), we have  $n \approx m$ . We will continue, unless stated otherwise, to deal with these two magnitudes separately in order to preserve their separate identity in particular in more complicated situations with more than a single trap and a single recombination centre. Chen and Pagonis<sup>(4)</sup> suggested a revised way of expressing the conditions leading to the expression reached by Halperin and Braner,<sup>(2)</sup> namely,

$$\left| \frac{dn_c}{dt} \right| \ll sn \exp(-E/kT), \quad n_c [A_n(N - n) + A_m m], \quad (6)$$

which basically means that the net rate of change of free electrons is significantly smaller than the rate of thermal elevation of electrons into the conduction band and the depletion of free electrons into the trap and centre together.

Following Halperin and Braner,<sup>(2)</sup> we get with these simplifying assumptions

$$I(T) = -\frac{dm}{dt} = sn \exp(-E/kT) \frac{A_m m}{A_m m + A_n (N - n)}. \quad (7)$$

This equation in two unknown functions,  $n$  and  $m$ , cannot be solved without further assumptions. As pointed out, as long as only one trap and one centre are involved, with the quasi-equilibrium equation mentioned we have  $n \approx m$ , and one gets an equation with one function,  $n$  only as shown by Kannunikov,<sup>(5)</sup>

$$I(T) = -\frac{dn}{dt} = sn \exp(-E/kT) \frac{A_m n}{A_m n + A_n (N - n)}. \quad (8)$$

If recombination dominates,  $A_m n \gg A_n (N - n)$  and one gets directly the Randall-Wilkins first-order equation

$$I(T) = -dn/dt = sn \exp(-E/kT). \quad (9)$$

As for the Garlick-Gibson assumption  $A_m = A_n$ , one gets from Equation (8) the second-order equation

$$I(T) = -\frac{dn}{dt} = \frac{s}{N} n^2 \exp(-E/kT). \quad (10)$$

It is worth mentioning that the condition  $A_m = A_n$  is not very likely to occur since we are talking about transitions into two entirely different entities in the crystal in hand, the imperfection responsible to the recombination centre and that associated with the trapping state. However, second-order behaviour can also be reached in another way. If retrapping dominates,  $A_n (N - n) \gg A_m n$ , Equation (8) reduces to

$$I(T) = -\frac{dn}{dt} = \frac{s A_m}{A_n N} n^2 \exp(-E/kT), \quad (11)$$

which is the same as Equation (10) except for the meaning of the pre-exponential factor.

TL peaks of first- and second-order have significantly different shapes. First-order peaks are asymmetric having the ascending range significantly broader than the descending range, whereas second-order peaks are nearly symmetric. In the literature, there are several reports on TL peaks, which have

intermediate symmetry properties. A very popular approach to deal with such peaks is the 'general order' equation (e.g. Chen<sup>(6)</sup>),

$$I(T) = -\frac{dn}{dt} = s' n^b \exp(-E/kT), \quad (12)$$

where  $b$  is usually between 1 and 2, and in some reports also  $b > 2$ . The advantage of this heuristic approach is that the solution of Equation (12) may yield any symmetry between those of the first- and second-order kinetics and beyond. The disadvantage is that there is no real physical basis to this presentation for  $b \neq 1, 2$  and also, that  $s'$ , the new pre-exponential factor has the odd units of  $\text{cm}^{3(b-1)} \text{s}^{-1}$ .

Another possible way of presenting intermediate cases is that of the mixed-order kinetics, developed by Chen *et al.*,<sup>(7)</sup>

$$I(T) = -\frac{dn}{dt} = s' n (n + c) \exp(-E/kT), \quad (13)$$

where  $s'$  the pre-exponential factor, has the same units as in the second-order equation, namely,  $\text{cm}^3 \text{s}^{-1}$ .

It should be noted that the explanation so far has been limited to the heating stage of TL and to a system with a single trapping state and a single kind of recombination centre. Let us consider briefly the relevant extensions, which will be further discussed in some detail in the coming chapters.

To begin with, in a luminescent material there are usually more than one kind of trap and/or one kind of recombination centre. In the heating stage, this would mean that one may expect more than one TL peak. The situation may be rather complex because we are not only considering an overlap of single peaks but also closer relation due to the possibility that electrons released from one trap may perform recombination with a number of centres, and in addition to retrapping in their original trap, they may also be trapped in other traps.

Another point of importance is that the read-out, which is due to heating in TL, is optical in OSL. In the basic equations mentioned above, the main point with regard to OSL is that in Equation (1),  $s \cdot n \cdot \exp(-E/kT)$  should be replaced by  $f n$  where  $f$  ( $\text{s}^{-1}$ ) is proportional to the intensity of the stimulating light.

Yet another crucial point to be considered has to do with the processes taking place during excitation. Let us consider in the Introduction the equations governing the process in the limited one trap one recombination centre case. The relevant transitions are seen in Figure 1, the meaning of the different parameters has been given above and the set of simultaneous

governing equations are

$$\frac{dn}{dt} = A_n (N - n) n_c - sn \exp(-E/kT), \quad (14)$$

$$\frac{dm}{dt} = B (M - m) n_v - A_m m n_c, \quad (15)$$

$$\frac{dn_c}{dt} = X - A_n (N - n) n_c - A_m m n_c, \quad (16)$$

$$\frac{dn_v}{dt} = \frac{dn}{dt} + \frac{dn_c}{dt} - \frac{dm}{dt}. \quad (17)$$

Obviously, if more traps and/or centres exist in the specimen, more equations of the same kind should be added to the set and solved simultaneously. Note that this set of equations governs the filling of traps and centres relevant to both TL and OSL. At the end of excitation one ends up with finite concentrations of free electrons,  $n_c$ , and free holes,  $n_v$ . If we wish to follow the experimental procedure of TL or OSL, we have to consider a relaxation time between the end of excitation and the beginning of heating or exposure to stimulating light. This is done in the simulations by setting  $X$  to zero and solving Equations (14–17) for a further period of time so that at the end, both  $n_c$  and  $n_v$  are negligibly small. The final values of  $n$ ,  $m$ ,  $n_c$  and  $n_v$  at the end of excitation are used as initial values of the relaxation stage and the final values of relaxation are used as the initial values for the read-out stage, Equations (1–3).

#### NON-LINEAR DOSE DEPENDENCE; SUPERLINEAR AND SUBLINEAR

For the applications in dosimetry and archaeological and geological dating, it is very advantageous to have linear dependence of the recorded TL and OSL on the dose. However, it is quite common to have super-linear (also called in the literature supralinear) dose dependence. Also, sublinear dose dependence occurs very frequently, in particular with high excitation doses where saturation effects associated with filling of the existing traps and recombination centres take place. In the framework of delocalised transitions, the superlinearity is associated with competing traps or recombination centres and their action during the excitation stage and/or the read-out phase.

The most common non-linearity has to do with sublinearity due to saturation effects that take place at relatively high doses when traps or centres are close to be filled up by carriers. More interesting situations are superlinear dose dependencies that occur under some conditions. To mention some, Cameron *et al.*<sup>(8)</sup> described the dose dependence of TL in LiF (TLD-100), which exhibited a rather broad linear dose

dependence followed by a steeper than linear dose range after which an approach to saturation was observed. Another sort of superlinearity was discovered by Tite<sup>(9)</sup> in ancient ceramics. The dose dependence curve found in this material is linear in a broad range except for the lowest doses where the TL starts increasing at a small rate with the dose and the rate increases gradually until it reaches a steady value. Another kind of superlinearity was reported by Halperin and Chen<sup>(10)</sup> who investigated the dependence of UV-irradiated semiconducting diamonds. A TL peak at  $\sim 250$  K was excited by UV light in the range of 300-400 nm with an initial dependence on the dose that could be presented as

$$I_{\max} = \alpha D^k, \quad (18)$$

where  $I_{\max}$  is the maximum intensity,  $D$  the applied dose and  $k$  a factor between 2 and 3 in the mentioned excitation range of 300-400 nm.

In order to have a uniform definition of superlinearity, Chen and McKeever<sup>(11)</sup> suggested the following. Let us denote by  $S$  the measured TL or OSL signal, be it the maximum intensity or the area under the curve in TL and the area in OSL, and  $D$  the absorbed dose. The derivative of the  $S$  function at a point  $D$  is  $dS/dD$  (or  $S'(D)$ ), and an increase of the derivative at a certain point is expressed by stating that  $d^2 S/dD^2$  (i.e.  $S''(D)$ ) is positive. Thus,  $d^2 S/dD^2 > 0$  is defined as representing ranges of superlinearity;  $d^2 S/dD^2 < 0$  characterises ranges of sublinearity and, of course,  $d^2 S/dD^2 = 0$  means a range of linearity. Chen and McKeever<sup>(11)</sup> have also defined the 'superlinearity index'  $g(D)$ ,

$$g(D) = \left[ \frac{DS''(D)}{S'(D)} \right] + 1. \quad (19)$$

As long as one deals with a range of increasing dose dependence, i.e.  $S'(D) > 0$ , it is obvious that  $g(D) > 1$  indicates superlinearity,  $g(D) = 1$  means a range of linearity and  $g(D) < 1$  signifies sublinearity. It is quite obvious that for the function given in Equation (18), one gets  $g(D) = k$  and, of course,  $k > 1$  indicates superlinearity.

The models explaining superlinear dose dependence of TL and OSL based on delocalised transitions have to do with competition between transitions into traps or centres, which may take place during either the excitation or during the read-out stage. In some cases, one may consider a combination of both excitation and read-out leading to strong superlinearity.

The first model explaining superlinearity has been suggested by Cameron *et al.*<sup>(8)</sup> (see their pages 168–174). This model proposed the creation of additional

traps by radiation and hypothesises a maximum possible trap density. Another model was given by Suntharalingam and Cameron<sup>(12)</sup> and further elaborated upon by Bowman and Chen.<sup>(13)</sup> These works deal with the filling of the relevant traps, which under the appropriate conditions are superlinear with the dose, and assumed that the total concentration of traps is not changed by the irradiation. Superlinearity is associated with the competition of electrons being trapped in the active traps and in competing, usually deeper traps. Let us consider the following intuitive somewhat simplified explanation. Suppose we have a system with  $N_1$  ( $\text{cm}^{-3}$ ) active traps and  $N_2$  ( $\text{cm}^{-3}$ ) competing traps. Let us assume that the trapping probability coefficient of the competitor,  $A_2$  ( $\text{cm}^3 \text{s}^{-1}$ ) is larger than that of the active trap,  $A_1$  ( $\text{cm}^3 \text{s}^{-1}$ ). At low doses, the excitation fills both traps linearly. However, at a certain dose the competing trap saturates and therefore more electrons are available to the relevant trap  $N_1$ . This means that the active trap will now be filled at a linear rate but faster than before. Nevertheless, the transition region from one linear range to the other would appear to be superlinear since this transition occurs continuously. Under the appropriate conditions, the measured signal, TL or OSL, follows the accumulated concentration of trapped electrons and thus, if the latter is superlinear, so is the former. Bowman and Chen have written the proper set of differential equations, made relevant simplifying assumptions and reached an expression that with the appropriate sets of parameters resulted in a dose-dependence curve, which starts linearly, continues superlinearly and then becomes sublinear while approaching saturation.

Another kind of superlinearity was reported first by Rodine and Land<sup>(14)</sup> who studied the dose dependence of TL peaks in  $\beta$ -irradiated  $\text{ThO}_2$ , which were found to be quadratic with the dose as of the lowest doses. These authors explained the effect qualitatively as the result of competition during heating. Kristianpoller *et al.*<sup>(15)</sup> further elaborated on competition during heating. Without competition, one may expect the area  $S$  under a glow peak to be proportional to  $\min(n_0, m_0)$  where  $n_0$  and  $m_0$  are the concentrations of electrons in traps and holes in centres, respectively, following excitation and relaxation prior to readout. Under regular conditions, the maximum TL intensity is approximately proportional to the area under the curve. Therefore, if  $n_0$  and  $m_0$  are linearly dependent on the dose of excitation, so is the measured TL intensity. However, Kristianpoller *et al.*<sup>(15)</sup> showed that in the presence of a strong competitor, the dependence of the area under the curve is

$$S \propto n_0 m_0, \quad (20)$$

and if  $n_0 \propto D$  and  $m_0 \propto D$ , then  $S \propto D^2$ .

In a later work, Chen *et al.*<sup>(16)</sup> combined the two models and showed, using numerical simulations, that with a model of two competing traps and one recombination centre, stronger than quadratic dose dependence may be reached, the main effect being related to competition during heating. The authors also reported on another model in which two competing recombination centres and one kind of trap are involved. A much weaker superlinearity associated mainly with competition during excitation is reported in the simulations of this model.

More recently, it has been shown that under certain circumstances, superlinearity of TL and OSL can take place even without competition. Chen *et al.*<sup>(17)</sup> used the simple OTOR energy level diagram (see Figure 1) and considered the situation where very high dose rates are being used. Referring to the above-mentioned condition for superlinearity,  $d^2n/dD^2$  being positive indicates superlinear dose dependence. Referring to the mentioned parameters in Figure 1 and Equations (14–16), the dependence of the occupancy of the traps on the dose can be given as

$$n = aD + bD^2 + O(D^3), \quad (21)$$

where

$$a = \frac{A_n N}{A_n N + A_m m_0}, \quad (22)$$

$$b = \frac{1}{2} \frac{A_m m_0 A_n N}{(A_n N + A_m m_0)^3} (A_m - A_n). \quad (23)$$

The coefficient  $b$  determines whether the initial response is superlinear. According to Equation (23), the behaviour is superlinear ( $b > 0$ ) if  $m_0 > 0$  and  $A_m > A_n$ . The initial dose dependence is expected to be linear if  $m_0 = 0$  or if  $m_0 > 0$  but  $A_m = A_n$ . Note that at higher doses, the  $D^3$  and higher order terms become significant but, on the other hand, saturation effects may set in. Yet another possible reason for a strong superlinear dose dependence may take place in cases of two-electron traps or two-hole centres.<sup>(18, 19)</sup>

## NON-MONOTONIC DOSE DEPENDENCE

In most cases, the dose dependencies of TL and OSL are monotonically increasing functions. In some cases, the reported dependence on the dose is such that the signal reaches a maximum at a certain dose and then the dose-dependence function declines. Cameron *et al.*<sup>(8)</sup> described the non-monotonic dependence of TL in LiF:Mg,Ti (TLD-100) as a function of  $^{60}\text{Co}$   $\gamma$ -ray dose. Jain *et al.*<sup>(20)</sup> reported on a significant decrease of the TL of peak V in LiF,

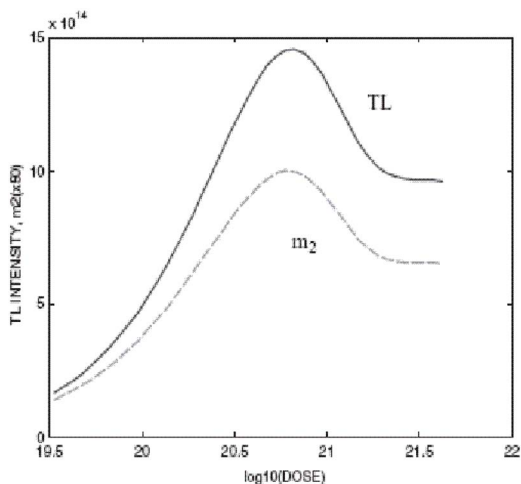


Figure 2: Simulated dose dependence of the maximum TL (solid line) and radiative-centre occupancy following irradiation,  $m_2$  (dashed line), when competition during irradiation dominates. (After Chen *et al.*<sup>(22)</sup>).

by a factor of  $\sim 2.5$  from the maximum, and ascribe it to radiation damage. Yukihiro *et al.*<sup>(21)</sup> reported on a slightly superlinear dependence up to  $\sim 10$  Gy of  $\beta$ -irradiation in  $\text{Al}_2\text{O}_3:\text{C}$  crystals. The peak reached a maximum value and declined at higher doses. Chen *et al.*<sup>(22)</sup> presented a model, which does not assume a radiation damage of destruction of trapping states. The authors use a model with two trapping states and two kinds of recombination centres. The competition over free charge carriers during excitation and heating was studied using both numerical simulations and intuitive considerations. Physically significant sets of trapping parameters were chosen, and the simulation of the three consecutive stages of the process, namely excitation, relaxation and heating was performed. An example of the results is shown in Figure 2. With the chosen set of parameters, the results show an increase of the TL maximum (solid line) with the dose up to a maximum at a 'dose' of  $\sim 7 \times 10^{20} \text{ m}^{-3}$ , followed by a decrease of  $\sim 35\%$  after which the maximum TL intensity levels off at higher doses. This behaviour is very similar to experimental results reported in some materials, e.g. Jain *et al.*<sup>(20)</sup> The dashed line shows the dependence of  $m_2$  on the dose, which seems to be the origin of the non-monotonic TL dose dependence. Pagonis *et al.*<sup>(23)</sup> used a similar model to explain the non-monotonic dose dependence of OSL, such as the results reported by Yukihiro *et al.*<sup>(24)</sup>

#### DOSE-RATE DEPENDENCE

In many studies of the dose dependence of TL and OSL, there is no distinction between changing the

dose by using different times of irradiation or by different dose rates with the same time of irradiation. Obviously, the dose applied to an examined sample may be varied by either changing the time of excitation or changing the applied dose rate. In principle, the dose rate and time of excitation are independent parameters. A 'trivial' dose-rate effect will take place when the temperature of the sample under excitation is rather high, say, in TL, quite close to the temperature of the TL peak observed following excitation. Such results have been reported e.g. by Facey.<sup>(25)</sup> Under these circumstances, the result in TL will be lower for a certain dose given by a small dose rate and a long time than in a situation where the same dose is applied by larger dose rate and shorter excitation time. However, a 'real' dose-rate effect of TL and OSL is sometimes reported in cases where the decay during excitation is negligible. This effect, reported in the literature, can be explained by models dealing with the interaction between trapping levels or recombination centres. It should be mentioned that when archaeological and geological dating is concerned, the natural dose rate may be as low as  $10^{-3} \text{ Gy/yr}$  ( $\sim 3 \times 10^{-11} \text{ Gy/s}$ ), whereas the laboratory dose rate used for comparison and calibration may be as high as several Gy/s. Groom *et al.*<sup>(26)</sup> reported on a strong genuine dose-rate effect in quartz when no thermal decay is involved. A decrease by a factor of  $\sim 5$  was observed with increasing dose rate, whereas the total dose was kept constant in powdered samples of Brazilian crystalline quartz irradiated by  $^{60}\text{Co}$   $\gamma$ -rays at dose rates in the range of 0.014–3.3 Gy/s. A smaller effect of the same kind in  $\text{CaSO}_4:\text{Dy}$  has been described by Hsu and Weng.<sup>(27)</sup> Shlukov *et al.*<sup>(28)</sup> criticised the archaeological and geological method of dating based on TL in quartz, stating that there is a difference of 8–9 orders of magnitude in the dose rate between natural and calibration irradiations, which may cause a serious error in the age evaluation. An unusual dose-rate effect has been reported by Valladas and Ferreira.<sup>(29)</sup> They detected separately three components in the emission of TL from quartz, namely, UV, blue and green. They found different behaviours of the three components while applying the same total dose of excitation at two dose rates, which are three orders of magnitude apart. The UV component was found to be nearly twice as large with the high dose rate as with the low one. With the green component, the low dose rate yielded  $\sim 10\%$  less emission than in the high one. As for the blue component, the low dose rate yielded  $\sim 50\%$  more TL than the high one.

Chen and Leung<sup>(30)</sup> have proposed a model to explain the mentioned dose-rate effect in which one component increases with the dose rate and the other decreases when the total dose remains constant. The model includes one kind of trapping state and two kinds of recombination centre, and it

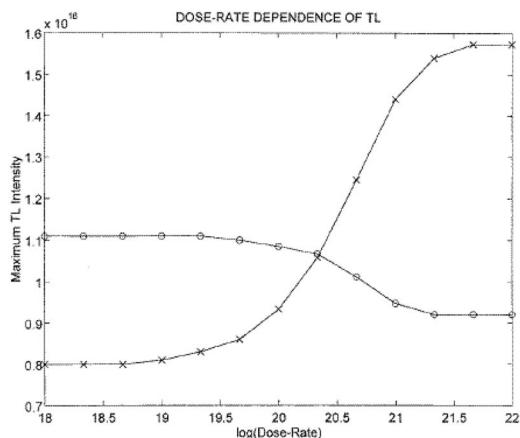


Figure 3: The dose-rate dependence of the TL maximum intensities of  $I_1(T)$  (crosses) and  $I_2(T)$  (circles) reached by simulations. (After Chen and Leung<sup>(30)</sup>).

simulates two spectral components, which depend on the dose rate in opposite ways. The relevant sets of coupled differential equations for the three stages of excitation, relaxation and read-out (heating) were solved sequentially, and the two emissions,  $I_1 = -dm_1/dt$  and  $I_2 = -dm_2/dt$ , were recorded, where  $m_1$  and  $m_2$  are the instantaneous occupancies of the two recombination centres. The simulated dose-rate dependence is given in Figure 3. The unusual behaviour, namely, that one spectral component increases with the dose rate and the other decreases can be clearly seen in the simulated results.

### PRE-DOSE SENSITISATION

For the applications in dosimetry as well as in archaeological and geological dating, it is evident that a constant sensitivity of the sample is desirable. In some instances, this is not the case. For example, the sensitivity of quartz samples to a 'test dose' increases significantly by  $\beta$  irradiation followed by high-temperature annealing. Originally, this is detrimental for the use of dating, but another method, based on the change of sensitivity with the dose has been developed. The theory behind the sensitisation effect will be described. In fact, in some cases even heating to high temperature alone and cooling back to room temperature may change the sensitivity of a sample to an applied test dose; however, the significant change results from the combination of rather high dose followed by high-temperature annealing.

Fleming,<sup>(31)</sup> Aitken<sup>(32)</sup> and others showed that the change of sensitivity of the  $\sim 110^\circ\text{C}$  peak in quartz could be used as a measure of the applied dose. These authors used  $\beta$  test-doses of  $\sim 0.01$  Gy and sensitising doses of the order of 1 Gy and measured the emission

of the quartz  $110^\circ\text{C}$  peak occurring at  $\sim 380$  nm. In addition, Zimmerman<sup>(33)</sup> reported on the UV reversal effect. If the quartz in hand, sensitised so as to yield high response to a test dose was illuminated by UV light in the range of 230–250 nm, the sensitivity was reduced significantly, nearly to the original one prior to irradiation followed by annealing. Another piece of relevant experimental evidence was reported by Fleming and Thompson.<sup>(34)</sup> If following a given irradiation of a sample the annealing is performed at different temperatures, different responses to a test dose were recorded, demonstrating the different sensitivities. In the case of the  $110^\circ\text{C}$  peak in quartz, the sensitivity increased following heating of up to  $500^\circ\text{C}$  and then decreased for higher temperatures. More work on the pre-dose effect in quartz has been reported by Martini *et al.*<sup>(35)</sup> who also suggested the identity of the relevant impurities taking part in the sensitisation of the  $110^\circ\text{C}$  peak.

Zimmerman<sup>(33)</sup> suggested the first model to account for the pre-dose sensitisation effect. The Zimmerman model deals with an electron trap T and two hole centres, R and L as is shown schematically in Figure 4. The recombination probability for trapping holes in R is assumed to be much larger than that in L, and thus, during irradiation practically all the free holes accumulate in R and the generated electrons congregate in T. However, this trap is rather shallow; it yields a TL peak at  $\sim 110^\circ\text{C}$  at a heating rate of  $5^\circ\text{C/s}$  and is emptied at room temperature within hours or may be readily emptied by heating to  $\sim 150^\circ\text{C}$ . R is assumed not to be very deep in the sense that it is close enough to the valence band so that heating to  $\sim 500^\circ\text{C}$  would release the holes into the valence band. Although their probability of trapping in L is rather low, at this high temperature, the net flow of holes through the valence band is from R to L. This is so since L is assumed to be much farther from the valence band, so that once a hole is captured at L, it cannot be thermally released back into the valence band. In this sense, R is a reservoir, which holds holes following the irradiation, prior to the thermal activation. According to Zimmerman, the increase of the concentration of holes in L represents an increase in the sensitivity since L is the luminescence centre.

Chen<sup>(37)</sup> proposed an amendment to the Zimmerman model. The experimental evidence has been that the measured response of the TL to a test dose is a monotonically increasing function of the concentration of trapped holes in L following the 'large' excitation followed by thermal activation on one hand, and also a monotonically increasing function of the magnitude of the test dose on the other hand. This requires the occurrence of a second trapping state for electrons, a deeper trap, which should act as a competitor to the released electrons during the read-out stage in which the sample is heated following the application of the test dose, and the emission is recorded at  $\sim 110^\circ\text{C}$ . Chen and Leung<sup>(36)</sup>

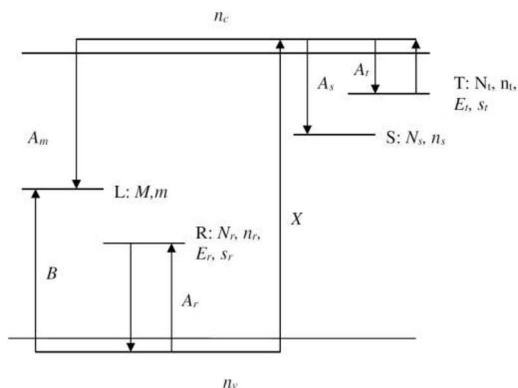


Figure 4: Energy level diagram for the explanation of the pre-dose effect of the 110°C peak in quartz. T is the trapping state, S is the competing electron trap, L is the luminescence centre and R the hole reservoir.  $n_c$  is the concentration of free electrons and  $n_v$  the concentration of free holes.  $X$  is the rate of production of free electrons and holes. (Redrawn from Chen and Leung<sup>(36)</sup>).

developed a mathematical model for the pre-dose effect in quartz, based on two electron and two hole trapping states. A schematic presentation of the model is shown in Figure 4. These authors simulated a typical sequence of experimental steps made during the pre-dose experimental technique consisting of a sequence of irradiations followed by annealing. By using physical arguments regarding the observed experimental behaviour of quartz, these authors arrived at good sets of parameters and successfully explained several experimental results associated with the pre-dose effect in quartz. Pagonis and Carty<sup>(38)</sup> showed that the model by Chen and Leung<sup>(36)</sup> could also be used to simulate successfully the complete sequence of experimental steps taken during the additive dose variation of the pre-dose technique. By solving the kinetic differential equations describing the model, Pagonis and Carty<sup>(38)</sup> demonstrated the mechanism of hole transfer from the reservoir to the luminescence centre, caused by heating to the activation temperature.

Pagonis *et al.*<sup>(39)</sup> simulated the sensitisation of quartz samples as a function of annealing temperature, yielding the thermal activation curve (TAC). They also used a modified Zimmerman model to simulate multiple TACs and the effect of UV radiation on the TL sensitivity (reversal) of quartz. These phenomena have analytical and diagnostic bearing in the application in the pre-dose dating technique.

## ANOMALOUS FADING

Methods have been developed for the evaluation of TL trapping parameters based on the shape of the

peaks, their shift with changing heating rates and in more complex situations, by deconvolution of tangled glow curves. Once these parameters are determined, one may expect certain decay times and decay functions. In some cases, 'anomalous' fading is observed, namely, the signal decays much faster than warranted by the trapping parameters. Understanding the process of fading of the TL or OSL signals is of great significance since in the applications in dosimetry and archaeological and geological dating, the stability or instability of the signal is of prime importance. Every TL peak may undergo thermal fading, which normally depends on the trapping parameters of the relevant trap and the temperature at which the sample is held following or during its excitation. In the simplest case of first-order kinetics the relevant parameters are obviously the activation energy  $E$  (eV) and the frequency factor  $s$  ( $s^{-1}$ ). The lifetime for decay at temperature  $T$  (K) is  $\tau = s^{-1} \exp(E/kT)$ , where  $k$  is Boltzmann's constant ( $eV \cdot K^{-1}$ ). The trapping parameters of a simple first-order TL peak,  $E$  and  $s$ , can rather easily be determined using the temperature of occurrence and the shape of the curve, and therefore, the expected decay time  $\tau$  can be found from this expression. For example, peak occurring at 500 K can be expected to be rather stable at room temperature ( $\sim 300$  K).

Several works reported on TL peaks that exhibited anomalous fading in a broad variety of materials since the early days of TL study. In 1950, Bull and Garlick<sup>(40)</sup> were apparently the first to report on this effect. They communicated on two UV excited peaks in diamond occurring at 400 and 520 K, which yielded significantly lower light levels if stored at 90 K before heating than if heated immediately after excitation. Hoogenstraaten<sup>(41)</sup> reported on the decay of light intensities at low temperature in ZnS samples. According to Hoogenstraaten, the effect is a result of the quantum-mechanical tunnelling of electrons from traps to recombination centres. Schulman *et al.*<sup>(42)</sup> found the effect in  $CaF_2:Mn$ . Kieffer *et al.*<sup>(43)</sup> reported a similar effect in organic glasses. In these cases, no temperature dependence of the anomalous fading was observed. On the other hand, Wintle<sup>(44)</sup> reported on the anomalous fading of various minerals at different temperatures and discussed its implications with regard to the dating of archaeological materials, in particular feldspars. Some studies of anomalous fading of TL and OSL in sanidine and other feldspars have been reported by Visocekas.<sup>(45)</sup> The anomalous fading was accompanied by red and infra-red (IR) emission of light, attributed to radiative tunnelling recombination. In a later work, Visocekas<sup>(46)</sup> has studied further the anomalous fading of TL in feldspars and found red emission at 710 nm, which is immune to the effect of anomalous fading and may therefore be utilised for use in dating. Visocekas *et al.*<sup>(47)</sup> have



studied also the afterglow of  $\text{CaSO}_4:\text{Dy}$  and showed that after the initial irradiation, a weak afterglow is seen for a long period of time with the same emission spectrum as the subsequently measured TL. The peak used for dosimetry in this material, occurring at  $\sim 250^\circ\text{C}$  decays to zero with time at room temperature and even at lower temperatures, almost independently of the temperature. These authors explain this anomalous fading as being the result of a quantum mechanical tunnelling effect. Templer<sup>(48)</sup> has studied the anomalous fading of zircon above room temperature and reported that localised transitions are responsible for the occurrence of the effect. On the other hand, at lower temperatures tunnelling seems to predominate. Tyler and McKeever<sup>(49)</sup> studied the anomalous fading of TL in oligoclase and concluded that the anomalous decay is more closely described by the local transition model of Templer than by quantum mechanical tunnelling.

As reported by several researchers, the initial fading rate of anomalous fading is quite rapid, followed by a slower decay at longer times. Visocekas and Geoffroy<sup>(50)</sup> investigated the fading of TL in calcite and concluded that the intensity  $I$  of the afterglow recorded during anomalous fading follows a hyperbolic law, i.e.  $I \propto 1/t$ , where  $t$  is the time. As explained earlier by Mikhailov,<sup>(51)</sup> a temperature independent hyperbolic dependence on time indicates that the underlying mechanism is tunnelling.

Chen and Hag-Yahya<sup>(52)</sup> considered the possibility that, in fact, anomalous fading might be in some instances a normal fading in disguise. They proposed that the observable TL peak may look significantly narrower than expected from the activation energy  $E$  and the frequency factor  $s$  of the peak due to competition with non-radiative centres. In their model, in addition to the radiative recombination centre  $M_2$ , two other non-radiative centres,  $M_1$  and  $M_3$  are assumed, the former with smaller recombination probability and the latter with larger probability. This causes the observed peak to be significantly narrower than otherwise expected by the  $E$  and  $s$  parameters. Let us consider a shape-based formula for evaluating the activation energy (see Chen<sup>(53)</sup>), which uses the full width of a single first-order TL peak,

$$E = 2.29kT_m^2/\omega, \quad (24)$$

where  $\omega = T_2 - T_1$  and, where  $T_1$  and  $T_2$  are the lower and higher half-intensity temperatures, respectively;  $T_m$  is the maximum temperature (in K);  $k$  is the Boltzmann constant ( $\text{eV}\cdot\text{K}^{-1}$ ) and  $E$  (eV) is the activation energy. Obviously, if a certain TL peak is narrower than expected due to any reason, the

apparent activation energy determined by Equation (24) will be larger than the real one. This may be the case here where due to the competition of the radiationless centres, the peak appears to be narrow and the effective activation energy is larger than the real one. Actually, similar results are expected with any peak-shape method as well as curve-fitting methods, which are utilising the same features of the glow peak. Chen and Hag-Yahya<sup>(52)</sup> have simulated glow peaks under these circumstances and found values of  $E_{app}$  significantly higher than the 'real' ones. Note that these authors chose the parameters such that the resulting glow peak had the symmetry of a first-order peak so that the observer would use the relevant first-order shape equation. For evaluating the expected lifetime, the Randall-Wilkins<sup>(2)</sup> equation for the maximum intensity of a first-order peak, which can be written as

$$s = \left[ \beta E / (kT_m^2) \right] \exp(E/kT_m), \quad (25)$$

and when one uses the apparent  $E_{app}$ , one gets the apparent  $s_{app}$ . Since the activation energy appears in the exponent, if large apparent activation energy is used then a value of  $s_{app}$  much larger than  $s$  can be expected. In a simulated example, Chen and Hag-Yahya<sup>(52)</sup> found an apparent lifetime based on the apparent energy and frequency factor, which was found to be four orders of magnitude larger than the real lifetime, based on the inserted  $E$  and  $s$  values.

Chen *et al.*<sup>(53)</sup> concluded that a possible explanation of the anomalous fading of TL has to do with competition during heating of the radiative centre with non-radiative centres. The competition narrows the peak significantly and the peak-shape methods yield large apparent activation energy, significantly larger than the actual one. As a result, the apparent frequency factor is found to be very much larger than the real one. Consequently, the apparent lifetime may be significantly higher than the real one. Thus, when one expects the longer, apparent lifetime and observes the latter real (thermal) fading, the measured fading is considered to be anomalous. In this sense, the effect is, actually, a normal fading in disguise.

#### ANOMALOUSLY HIGH EFFECTIVE ACTIVATION ENERGIES AND FREQUENCY FACTORS

In some materials, anomalously high values of the main trapping parameters, the activation energy and the frequency factor have been reported. The possible reasons for this occurrence will be discussed here. As pointed out by several authors, the values of the frequency factor  $s$  are expected to be in the range of  $10^8$ – $10^{13} \text{ s}^{-1}$  (see e.g. Lax<sup>(54)</sup>). According

to Mott and Gurney,<sup>(55)</sup>  $s$  should be of the order of magnitude of the Debye frequency, which is associated with the number of times per second that the trapped electron interacts with the phonons. Lower values of the frequency factor as well as higher values have been reported in the literature. In a number of published TL peaks, the determined  $s$  values exceed significantly the expected physical values of up to  $\sim 10^{13} \text{ s}^{-1}$  and can probably be considered as effective frequency factor rather than 'real'. The best-known case is that of peak 5 occurring at  $\sim 480 \text{ K}$  in LiF:Mg,Ti (TLD-100). The experimentally evaluated  $E$  and  $s$  as reported in the literature vary a lot, depending mainly on the method used for calculating the parameters. When isothermal decay methods were used, values of  $E \sim 1.25 \text{ eV}$  and  $s \sim 10^{10} - 2 \times 10^{12} \text{ s}^{-1}$  were found (see e.g. Zimmerman *et al.*,<sup>(56)</sup> Blak and Watanabe,<sup>(57)</sup> Yossian *et al.*<sup>(58)</sup>). However, for the same peak, Taylor and Lilley<sup>(59)</sup> reported an activation energy of  $2.06 \text{ eV}$  and a frequency factor of  $2 \times 10^{20} \text{ s}^{-1}$ , which they found using a peak-shape method. Gorbics *et al.*<sup>(60)</sup> used the method of various heating rates and reported for peak 5 values of  $E = 2.4 \text{ eV}$  and  $s = 1.7 \times 10^{24} \text{ s}^{-1}$ . Pohlit<sup>(61)</sup> reported an exceedingly high values of  $E = 3.62 \text{ eV}$  and  $s = 10^{42} \text{ s}^{-1}$  for the same peak 5 in LiF.

Fairchild *et al.*<sup>(62)</sup> suggested that the high  $s$  value of peak 5 in LiF as well as other unusually high  $s$  values may result from a complex kinetics and that the apparent first-order behaviour is a special case or approximation of a much more complex situation. An international effort to compare results in LiF by numerical deconvolution of the glow curve showed unambiguously these very high values of  $E$  and  $s$  (see Bos *et al.*<sup>(63)</sup>) for peak 5 in LiF.

Extremely high values of the frequency factor have also been determined for other materials. For example, Bilski *et al.*<sup>(64)</sup> reported an activation energy of  $E = 4.47 \text{ eV}$  and a frequency factor of  $s = 5.6 \times 10^{28} \text{ s}^{-1}$  for a peak at  $\sim 400^\circ\text{C}$  in LiF:Mg, Cu, P. Mandowska *et al.*<sup>(65)</sup> found values of  $E = 2.58 \text{ eV}$  and  $s = 3.5 \times 10^{24} \text{ s}^{-1}$  in a peak at  $501 \text{ K}$  in KCl.

It is agreed by researchers that the occurrence of such high apparent activation energies and very high effective frequencies are associated with the existence of very narrow TL peaks. As explained in the section 'Anomalously high effective activation energies and frequency factors' above with regard to anomalous fading, if by some reason a TL peak is very narrow, the effective activation energy determined by any peak-shape method or best-fit method will be much larger than otherwise expected. Consequently, the effective frequency factor is evaluated to be several orders of magnitude higher than the real one. Chen and Hag-Yahya<sup>(66)</sup> adopted the same model of competition with radiationless centres utilised to explain the anomalous fading and showed that with

an appropriate choice of the other parameters, when entering values of  $E = 1.2 \text{ eV}$  and  $s = 2.5 \times 10^{11} \text{ s}^{-1}$ , a peak with first-order features was simulated, with a symmetry factor of 0.42, and its analysis yielded effective values of  $E_{\text{eff}} = 2.24 \text{ eV}$  and  $s_{\text{eff}} = 9.3 \times 10^{21} \text{ s}^{-1}$ . It should be noted that the adjacent peaks associated with the two competing centres may not be radiationless but rather, they can be separated from the peak in question by deconvolution or by optical separation and the apparent high values of  $E$  and  $s$  be found. This may possibly be the case in LiF:Mg,Ti (TLD-100) where a number of other peaks are known to occur in the combined glow curve above and below peak 5 at  $\sim 480 \text{ K}$ .

As an alternative to the explanation of the occurrence of very narrow TL peaks leading to very high values of the mentioned parameters, Mandowski<sup>(67)</sup> presented a semi-localised transitions model, which in some cases leads to a cascade detrapping (CD) mechanism. The CD mechanism produces very narrow TL peaks, which are also well described by first-order kinetics with very high effective activation energies and exceedingly high-frequency factors.

## ANOMALOUS STABILITY

In the 'normal' cases, one expects that the excited signal will decay exponentially with time, with a certain decay time constant. In some cases, the signal decays approximately exponentially at relatively short times, but more slowly at longer periods of time. If one relies on the shorter-time behaviour, the longer-time decay may look like anomalous stability. The possible reason for this behaviour will be discussed here. In the graphic presentation of the decay, if the results are shown on a semi-logarithmic scale, the exponential decay looks like a straight line. In some cases, this presentation yields a straight line only at the beginning, and the line gets concave at longer periods of time, which means that the decay is slower than exponential. Some experimental results of such slower than exponential decay are the following. Sharon *et al.*<sup>(68)</sup> presented the results of the isothermal decay of a glow peak occurring at  $105^\circ\text{C}$  when the sample is held at temperatures in the range of  $65-75^\circ\text{C}$ . The lines on a semi-log scale started being nearly linear, indicating an initial nearly exponential decay, but continued being slower than linear on this scale, exhibiting a concave curve. Kathuria and Sunta<sup>(69)</sup> presented results of the isothermal decay of peaks 4 and 5 in LiF TLD-100 samples and showed similar concave curves at different temperatures. Kitis *et al.*<sup>(70)</sup> showed results of the same kind in samples of  $\text{MgB}_4\text{O}_7\text{:Na}$  and  $\text{LiB}_4\text{O}_7\text{:Cu}$ .

The question of whether the decay of TL and OSL is exponential or slower is of primary importance in dating of archaeological and geological samples when

the time scale may be as high as thousands of years and more. The behaviour of the short-time decay mentioned indicates that such slower than exponential decay of TL and OSL is possible. Chen and Pagonis<sup>(71)</sup> studied theoretically the possible decay when the simple model used was of one trap and one centre and the trapping parameters are such that the decay is on a scale of thousands years. With the parameters used, in a small sample such as a grain of quartz used for dating, the electrons are released thermally from the trap at ambient temperature at a very slow rate, one at a time. Therefore, these authors preferred to follow the kinetics of the process using a Monte Carlo algorithm. They followed the transitions of electrons from the trap into either the recombination centre or back to the trap by retrapping at a constant temperature of 300 K and recorded the remaining number of electrons in the traps following long times of slow decay. Note that the choice of  $N = 10^7$  traps is realistic for a fine grain, which has a size of  $\sim 100 \mu\text{m}$  and a volume of  $\sim 10^{-6} \text{cm}^3$  if the concentration of the traps is  $10^{13} \text{cm}^{-3}$ . The assumption in this example is that initially 10% of the traps are occupied, and therefore, the initial number of electrons in traps is  $10^6$ . Note also that with the mentioned choice of the trapping parameters, the rate of thermal release of electrons is less than one per day. An example of the simulated results is shown in Figure 5; the relevant parameters are given in the caption. The simulated results go to 14 000 years and are shown on a semi-log scale. The results up to  $\sim 500$  years form a nearly straight line, which means that the decay is practically exponential. However, due to the increasing effect of retrapping, from 500 years on, the line curves quite significantly. Although the exponential goes down by three orders of magnitude in  $\sim 2000$  years, the slower simulated line decreases by less than three orders of magnitude in 14 000 years. Therefore, if one determines the expected fading time by the initial exponential, one observes an apparent effect of anomalous stability since the real decay is strongly sub-exponential. It is worth mentioning that in a recent work, Chen and Pagonis<sup>(72)</sup> added to the simple OTOR model a competing deeper trap and found that with the choice of the appropriate parameters, the decay tends to be closer to exponential. Thus the tendency to anomalous stability is less likely to take place since the occurrence of competing traps is often expected. This point is related to the discussion in the section ‘Ubiquity of first-order TL peaks’ below that shows that first-order TL peaks usually occur in the presence of competing traps. Finally, another model by Chen *et al.*,<sup>(73)</sup> dealing with TL resulting from two-stage thermal stimulation also resulted in the possibility of having anomalous stability.

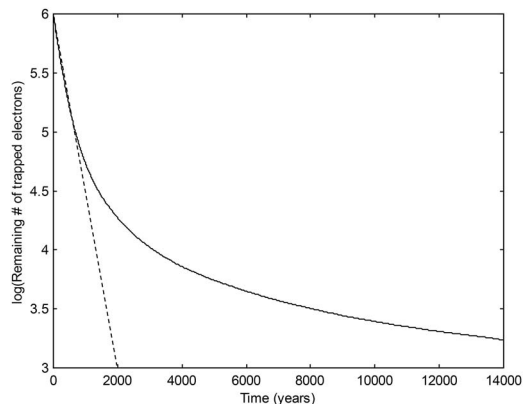


Figure 5: Time dependence of the remaining concentration of electrons in traps, simulated by the Monte Carlo method. The parameters are  $N = 10^7$ ;  $n_0 = 10^6$ ;  $E = 1.3 \text{ eV}$ ;  $s = 10^{12} \text{ s}^{-1}$ ;  $T = 300 \text{ K}$ ;  $A_m = 10^{-8} \text{ cm}^3 \text{ s}^{-1}$  and  $A_n = 10^{-10} \text{ cm}^3 \text{ s}^{-1}$ . The straight dashed line represents the initial exponential decay at the rate determined by the  $E$  and  $s$  values. (After Chen and Pagonis<sup>(71)</sup>).

## CONCENTRATION QUENCHING

For low-energy excitation, the TL and OSL phenomena depend on the impurities and defects in the host crystal. At first sight, one may expect that the higher the concentration of imperfections, the higher the resulting luminescence in response to a given excitation. In many cases, this indeed is the case, but in some instances, when the impurity concentration increases, the response to a given dose reaches a maximum and then declines with higher concentrations. This effect is termed ‘concentration quenching’. The effect in luminescence has first been described by Johnson and Williams.<sup>(74)</sup> They reported on the dependence of luminescence efficiency on Mn impurity in  $\text{ZnF}_2$ , which showed an increase with the concentration up to a certain fraction of the activator, yielded a maximum at this concentration and a decline at higher concentrations. Making some assumptions regarding the activator and host lattice their model yielded a peak-shaped behaviour of the luminescence efficiency as a function of the activator concentration. Ewles and Lee<sup>(75)</sup> suggested an amendment to this model in luminescence while explaining its occurrence in yellow and UV emission in  $\text{CaO:Bi}$  and in  $\text{CaO:Pb}$ . This non-monotonic dependence on the impurity concentration has later been found in other materials. Schulman *et al.*<sup>(76)</sup> reported on concentration quenching of luminescence in  $\text{KCl:Tl}$ , which exhibited a maximum at  $\sim 0.1$  mol per cent. Van Uitert<sup>(77)</sup> described the effect in  $\text{CaWO}_4:\text{Tb}$  and  $\text{CaWO}_4:\text{Eu}$ . In the latter material, the maximum occurred at different concentrations for different luminescence emission wavelengths.

The concentration quenching of TL has later been reported by several researchers. Medlin<sup>(78)</sup> described the TL properties of calcite and reported on concentration quenching of the 350 K peak associated with  $Mn^{++}$ . In a later work, Medlin<sup>(79)</sup> communicated on concentration quenching of four peaks in  $Mn^{++}$  doped dolomite, at 330, 380, 500 and 600 K with different concentrations between 0.001 and 0.003 mol fraction of  $Mn^{++}$ . Rossiter *et al.*<sup>(80)</sup> reported on the concentration dependence of peak 5, at 210°C in  $LiF:Ti$  where concentration quenching was found. Wachter<sup>(81)</sup> has studied the dependence of the sensitivity of  $LiF:Mg,Ti$  (TLD-100) on the ratio of the two dopants  $Mg/Ti$  and found a peak-shaped dependence with a maximum at a ratio of  $\sim 0.32$ . Lai *et al.*<sup>(82)</sup> investigated the TL of  $ZrO_2$  doped with  $Yb_2O_3$  and found concentration quenching with a maximum at 5 mol%. Tajika and Hashimoto<sup>(83)</sup> investigated the blue TL in synthetic quartz with aluminium impurity and found a maximum TL intensity with 10 ppm of aluminium. Vij *et al.*<sup>(84)</sup> reported on the TL of UV-irradiated Ce doped SrS nanostructures in which they found a maximum sensitivity at a dopant concentration of  $\sim 0.5$  mol%.

Chen *et al.*<sup>(85)</sup> proposed a possible model to explain the concentration quenching of TL intensity; a model specific to TL. The model includes three trapping states and one recombination centre (3T1C model). The assumption made is that the three traps have a constant concentration, and the variable concentration is that of the recombination centre. Another assumption made is that the initial occupancy of the centre is not zero. These authors wrote the relevant set of six simultaneous differential equations, which govern the stages of excitation, relaxation and heating. Two TL peaks are thus simulated using the assumption that the initial concentration of holes in centres is not zero. For the simulations, it is assumed that 10% of the centres are full prior to the excitation. The results yield the concentration dependence of the area under each of the two simulated peaks reached by solving numerically the mentioned sets of equations. The maximum intensities of the two peaks occur at different concentrations, similarly to the experimental results in  $Pb^{++}$  doped calcite and  $Mn^{++}$  doped dolomite. The authors support these results by approximate analytical derivations. An example of the simulated results is shown in Figure 6. The authors point out that the concentration quenching effect of a single TL peak, an effect found in several materials, can be simulated by a simpler model of two traps and one recombination centre (2T1C).

#### ANOMALOUS HEATING-RATE EFFECT

The ‘intensity’ of TL may be defined as the emitted light intensity per second or per degree. If the heating

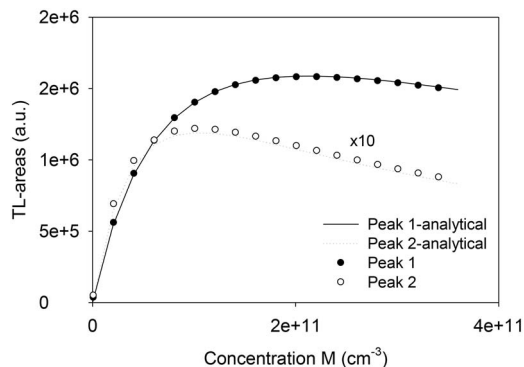


Figure 6: Simulated results of the concentration dependence of the areas under two peaks, at 91 and 220°C. (After Chen *et al.*<sup>(85)</sup>).

rate is increased, the former increases nearly linearly with the heating rate, whereas the latter decreases slightly with the heating rate. In some cases, the latter behaves ‘anomalously’, namely the intensity (per degree) increases with the heating rate. In some instances, two TL peaks in the same sample behave in opposite ways, one increasing with the heating rate and one decreasing. A model explaining the phenomenon is discussed here along with its possible relation to the thermal quenching effect.

In most cases, a constant heating rate, denoted by  $\beta$  (K/s) is used for the recording of TL. In practically all cases, the TL glow peak shifts to higher temperature with increasing heating rate (see e.g. Hoogenstraaten<sup>(41)</sup>). This can rather easily be demonstrated for the simple case of first-order kinetics. The equation for the TL maximum is Equation (25) mentioned above, which can be written as

$$\beta = (sk/E) T_m^2 \exp(-E/kT_m). \quad (25')$$

When the heating rate  $\beta$  increases, the right-hand side must increase by the same amount. However, since  $T_m^2 \exp(-E/kT_m)$  is an increasing function of  $T_m$ , its increase implies that  $T_m$  must increase. Furthermore, it has been shown (see e.g. Chen and Winer<sup>(86)</sup>) that although in more complex cases of TL kinetics Equation (25) is only an approximation, the shift of TL peaks to higher temperatures with increasing heating rate seems to be a general property.

Chen and Pagonis<sup>(87)</sup> discussed in detail the distinction between two alternative presentations of TL. As an example, they considered the simple example of first-order kinetics as given in Equation (9) above. Note that, as long as a constant heating rate is used, the transformation between  $I(T)$ , the dependence on temperature as given in Equation (9) and  $I(t)$ , the dependence on time, is straightforward. As is, the

units of  $I(T)$  or  $I(t)$  as in Equation (9) are  $\text{cm}^{-3}\text{s}^{-1}$ , whereas the real intensity is given in photons per second or emitted energy per second. As reported before (e.g. Kumar *et al.*<sup>(88)</sup>), when increasing the heating rate, the maximum intensity of TL in photons per second increases nearly proportionally to the heating rate. The area under the curve must remain the same independently of the heating rate and the simple explanation for the increased intensity is that with fast heating rate, the peak gets much narrower on the time scale. An alternative, rather common presentation is reached by normalising the intensity as defined in Equations (9–13) by dividing it by the heating rate  $\beta$ . Unfortunately, the normalised intensity is also usually termed in the literature ‘intensity’. This magnitude is usually plotted as a function of temperature rather than time. The area under the curve in this presentation remains constant with different heating rates (see e.g. Kumar *et al.*<sup>(88)</sup>) and this normalised intensity, which is  $I(T) = -dn/dT$  has a somewhat decreasing maximum value associated with a slight broadening of the peak with increasing heating rate.

Wintle<sup>(89)</sup> reported on thermal quenching of TL in quartz, which is the decrease in luminescence intensity with the rise in temperature. It should be mentioned that this effect had been described before for other luminescence effects (e.g. Curie<sup>(90)</sup>). Two possible models have been offered for the explanation of the luminescence effect. According to Mott and Seitz (Seitz<sup>(91)</sup>; Mott and Gurney<sup>(92)</sup>), radiative and non-radiative transitions compete within the surrounding of the luminescence centres as is the case in KCl(Tl). The luminescence efficiency decreases with increasing temperature due to a reduction in the quantum efficiency of the luminescence centres. An alternative explanation has been suggested by Schön<sup>(93)</sup> and Klasens.<sup>(94)</sup> Their model assumes that the holes in the centres may be thermally released into the valence band, thus decreasing the number of holes available for recombination with thermally stimulated electrons. Note that a similar model with traps and centres releasing electrons and holes respectively, simultaneously, has later been discussed by Lawless *et al.*<sup>(95)</sup> and explained the possibility of the occurrence of duplicitous TL peaks.

It has been reported by a number of authors (e.g. Nansjundaswamy *et al.*<sup>(96)</sup>; Rasheedy and Zahran<sup>(97)</sup>; Subedi *et al.*<sup>(98)</sup>; Kalita and Wary<sup>(99)</sup>) that in some materials, the decrease of the maximum of the normalised TL with the heating rate was significantly faster than the slight decrease described above. The explanation given has been that since the peak shifts to higher temperature with the increased heating rate, the intensity decreases due to the thermal quenching. Therefore, the area under the normalised curve is not constant but rather; it decreases with increasing heating rate.

In later works, a number of reports on an inverse, anomalous heating-rate effect have been published. Kitis *et al.*<sup>(100)</sup> have reported on a heating-rate effect in fluoroapatite in which the maximum normalised TL intensity and the area under the curve increased with the heating rate. Pradhan *et al.*<sup>(101)</sup> have described a similar effect in LiF:Mg, Cu, Si. Bos *et al.*<sup>(102)</sup> described the effect in  $\text{YPO}_4:\text{Ce}^{3+}, \text{Sm}^{3+}$ . Delice *et al.*<sup>(103)</sup> reported on the same effect in  $\text{Ti}_2\text{GaInS}_4$ , and Benabdesselam *et al.*<sup>(104)</sup> found it in Ge-doped silica-based optical fibre. Delice *et al.*<sup>(105)</sup> later described the results of TL in GaS. These authors reported on the behaviour of two peaks at different heating rates. Although the lower-temperature normalised peak decreased with the heating rate, the higher-temperature one increased with  $\beta$ .

Chen and Pagonis<sup>(87)</sup> presented a model, which explains the anomalous heating-rate effect. In a similar way to the Schön-Klasens model, the model is based on delocalised transitions only. In addition to the occurrence of an electron trap and a hole centre, one assumes the participation of a hole reservoir, which competes with the other levels for electrons and participates in the process during both the excitation and the read-out stages. The authors assume that the reservoir is close enough to the valence band so that holes may be thermally released into the valence band in the same temperature range in which electrons are raised into the conduction band. To some extent, this model is similar to the one used to explain the pre-dose effect (see section ‘Pre-dose sensitisation’ above). Simulations with this model show that, with certain sets of trapping parameters an increase of the heating rate results in an increase in the area under the normalised TL curve. Chen and Pagonis<sup>(87)</sup> show that by assuming an inversion in the roles of the recombination centre and the reservoir so that the recombination of free electrons with holes in the reservoir is assumed to be radiative and the other recombination is radiationless, one gets opposite results. Here, increasing the heating rates causes a significant decrease in the area under the TL curve, which may be an alternative explanation of the well-known thermal-quenching heating-rate effect of TL.

Chen and Pagonis<sup>(87)</sup> further used this model to explain the mentioned results by Delice *et al.*<sup>(105)</sup> in which in GaS, the area under one TL peak increased with the heating rate and that under the other peak decreased. Using the mentioned model with two centres and one trap, Chen and Pagonis chose a set of relevant parameters and along with the assumption that holes may be released thermally from the centre  $M_2$ , recorded the sum of the two peaks reached by transitions of electrons from the conduction band into the two centres,  $M_1$  and  $M_2$ . The results of this simulation are shown in Figure 7. These results are qualitatively

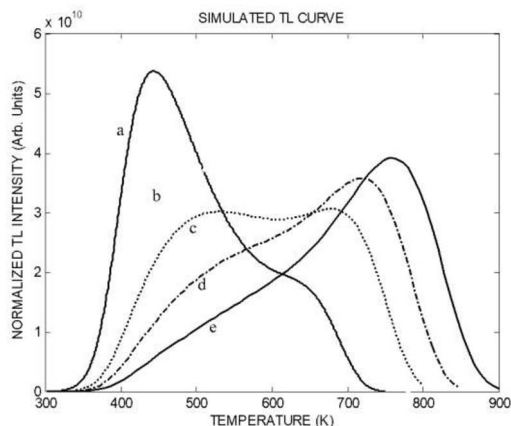


Figure 7: Simulated TL curves assuming that both transitions into  $M_1$  and  $M_2$  are radiative. The parameters used:  $E_1 = 0.9$  eV;  $E_2 = 0.7$  eV;  $s_1 = 10^{11}$  s $^{-1}$ ;  $s_2 = 10^{13}$  s $^{-1}$ ;  $n = 10^{14}$  cm $^{-3}$ ;  $M_1 = 10^9$  cm $^{-3}$ ;  $M_2 = 10^{14}$  cm $^{-3}$ ;  $A_{m1} = A_{m2} = 10^{-8}$  cm $^3$  s $^{-1}$ ;  $B_1 = 10^{-7}$  cm $^3$  s $^{-1}$ ;  $B_2 = 10^{-10}$  cm $^3$  s $^{-1}$ ;  $A_n = 10^{-7}$  cm $^3$  s $^{-1}$ ; and  $X = 10^{12}$  cm $^{-3}$  s $^{-1}$ . The heating rates are from 0.5 to 8 Ks $^{-1}$  in curves (a–e). (After Chen and Pagonis<sup>(87)</sup>).

very similar to the mentioned experimental results in GaS crystals reported by Delice *et al.*<sup>(105)</sup>

### UBIQUITY OF FIRST-ORDER TL PEAKS

As described in the Introduction, the OTOR model leads to first-order kinetics when recombination dominates and to second order when retrapping dominates or when the recombination and retrapping probability coefficients are equal. Of course, intermediate cases are possible as mentioned above. However, in vast experimental results, first-order peaks are abundant and there is no convincing evidence that recombination probability is usually significantly larger than the retrapping probability. Lewandowski and McKeever<sup>(106)</sup> stated that the first-order processes dominate in nature. Sunta *et al.*<sup>(107)</sup> suggested that the apparent dominance of first-order kinetics in nature is usually due to slow retrapping, but in multiple-trap system models, it may occur under fast retrapping as well. Further examples of the dominance of first-order kinetics have been given by Bos<sup>(108)</sup> and by Abd El-Hafez *et al.*<sup>(109)</sup> Some researchers described the prevalence of first-order shaped peaks in both TL and thermally stimulated conductivity and mentioned the competition with deep traps as the reason. These include Haering and Adams,<sup>(110)</sup> Dussel and Bube,<sup>(111)</sup> Böhm and Scharmann,<sup>(112)</sup> Simmons and Taylor,<sup>(113)</sup> Agersap Larsen *et al.*<sup>(114)</sup> and Opanowicz.<sup>(115)</sup>

Pagonis and Kitis<sup>(116)</sup> reported on the ubiquity of first-order kinetics based on multiple competition

processes. In an interactive multitrapping system model, they chose sets of parameters at random within the reasonable ranges, solved the equations to get glow curves and monitored the effective order of kinetics of the peaks. With a 1000 sets of parameters, they got a distribution of effective kinetic orders weighted strongly toward first order. The distribution has a mean value of the effective order of  $b = 1.08$  and a standard deviation of  $\sigma = 0.16$ . The authors ascribe the nearly first-order property to the competition between traps.

Chen and Pagonis<sup>(117)</sup> followed this work by using a model with several trapping states, and showed analytically under what circumstances the peaks in a series could be expected to be of first order. In particular, they distinguished between the lower temperature peaks in a series and the high temperature one. Basically, in such a series of peaks, the lower temperature peaks occur when the active trap has competing deeper traps that cause the effective kinetics to be of first order. With the last peak in such a series, the thermally released electrons do not ‘see’ a competitor and the shape of the peak tends to be that of a second-order curve and as shown by Chen and Pagonis<sup>(117)</sup> in some cases, its shape indicates an apparent order larger than two. These authors developed approximate expressions for the shape of the peaks in such a series and showed a number of examples of simulated glow curves based on such a model with a number of trapping states and one or more recombination centres. An example is shown in Figure 8, the parameters are given in the caption. The symmetry factors were found to be  $\mu_{g1} = \mu_{g2} = 0.42$ ;  $\mu_{g3} = \mu_{g4} = 0.41$ ;  $\mu_{g5} = 0.49$ . It is obvious that the first four peaks look like first-order curves and the fifth one is rather close to look like a second-order peak.

Chen and Pagonis<sup>(117)</sup> have also shown that even in the more complex and realistic situation in which multiple trapping states as well as a number of recombination centres take part in the TL process, the prevalence of first-order peaks is still expected in spite of the very intricate processes involving simultaneously several traps and centres. This is so even when retrapping is significantly stronger than recombination. As pointed out above, this may be the main explanation for the experimentally known fact that many TL peaks from different materials tend to have the first-order symmetry. It is also possible that in real-life cases, high-temperature peaks that are not measurable due to black-body radiation background may contribute, due to the competition of their deep traps, to the first-order appearance of the preceding peaks. The high-temperature peaks may possibly have second- or even higher-order features, but since they are not measurable, the impression that first-order peaks are so ubiquitous may be further strengthened.

Chen and Pagonis<sup>(117)</sup> concluded by reporting that in the example given in Figure 8 as well as several

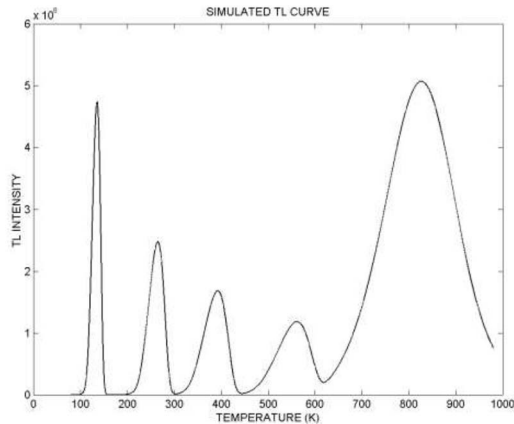


Figure 8: Simulated glow curve using a model with one recombination centre and 5 trapping states.  $M = 10^{12} \text{ cm}^{-3}$ ;  $B = 10^{-10} \text{ cm}^3 \text{ s}^{-1}$ ;  $A_i = 10^{-9} \text{ cm}^3 \text{ s}^{-1}$ ;  $E_i = (0.3, 0.6, 0.9, 1.3, 1.8) \text{ eV}$ ;  $A_m = 10^{-11} \text{ cm}^3 \text{ s}^{-1}$ ;  $s_i = 10^{11} \text{ s}^{-1}$ ;  $X = 2 \times 10^{10} \text{ cm}^{-3} \text{ s}^{-1}$ ;  $N_i = 10^{10} \text{ cm}^{-3}$  for  $i = 1, \dots, 4$ ; and  $N_5 = 10^{11} \text{ cm}^{-3}$ . (After Chen and Pagonis<sup>(117)</sup>).

other examples of the same sort, the results of the activation energies found by peak-shape methods applied to the peaks in the series were found to match in most cases rather accurately the parameters used in the simulations. The effective frequency factors were found to be within a factor of  $< 2$  of the original  $s$  value in the example given and other examples, which can be considered as a good agreement. This point is important because if one wants to consider the stability of a TL peak, say, at room temperature, the knowledge of the relevant activation energy and frequency factor is of importance.

Finally, Benavente *et al.*<sup>(118)</sup> have recently shown by simulations that the prevalence of first-order occurs not only when the individual peaks in a series are well separated but also when the components of an entangled glow curve are numerically deconvoluted.

## REFERENCES

1. Randall, J. T. and Wilkins, M. H. F. *The phosphorescence of various solids*. Proc. Roy. Soc. Lond. A **184**, 347–365 (1945).
2. Halperin, A. and Braner, A. A. *Evaluation of thermal activation energies from glow curves*. Phys. Rev. **117**, 408–415 (1960).
3. Garlick, G. F. J. and Gibson, A. F. *The electron-trap mechanism of luminescence in sulphide and silicate phosphors*. Proc. Phys. Soc. **60**, 574–590 (1948).
4. Chen, R. and Pagonis, V. *On the quasi-equilibrium assumptions in the theory of thermoluminescence (TL)*. J. Lumin. **143**, 734–740 (2013).
5. Kannunikov, I. A. *Reaction order of thermally stimulated recombination*. J. Appl. Spect. **28**, 597–599 (1978).
6. Chen, R. *Glow curves with general-order kinetics*. J. Electrochem. Soc. **116**, 1254–1257 (1969).
7. Chen, R., Kristianpoller, N., Davidson, Z. and Visocekas, R. *Mixed first and second order kinetics in thermally stimulated processes*. J. Lumin. **23**, 293–303 (1981).
8. Cameron, J. R., Suntharalingam, N. and Kenney, G. N. *Thermoluminescence Dosimetry*. (The University of Wisconsin Press, Madison, Wisconsin) (1968).
9. Tite, M. S. *Thermoluminescence dating of ancient ceramics: a reassessment*. Archaeometry **9**, 155–169 (1966).
10. Halperin, A. and Chen, R. *Thermoluminescence in semiconducting diamonds*. Phys. Rev. **148**, 839–845 (1966).
11. Chen, R. and McKeever, S. W. S. *Characterization of nonlinearities in the dose dependence of thermoluminescence*. Radiat. Meas. **23**, 667–673 (1994).
12. Suntharalingam, N. and Cameron, J. R. *Thermoluminescence response of lithium fluoride to radiations with different LET*. Phys. Med. Biol. **14**, 397–410 (1969).
13. Bowman, S. G. E. and Chen, R. *Superlinear filling of traps in crystals due to competition during irradiation*. J. Lumin. **18**, 345–348 (1979).
14. Rodine, E. T. and Land, P. L. *Electronic defect structure of single crystal  $\text{ThO}_2$  by thermoluminescence*. Phys. Rev. **B4**, 2701–2724 (1971).
15. Kristianpoller, N., Chen, R. and Israeli, M. *Dose dependence of thermoluminescence peaks*. J. Phys. D: Appl. Phys. **7**, 1063–1074 (1974).
16. Chen, R., Fogel, G. and Lee, C. K. *A new look at the models of the superlinear dose dependence of thermoluminescence*. Radiat. Prot. Dosimetry **65**, 63–68 (1996).
17. Chen, R., Lawless, J. L. and Pagonis, V. *Intrinsic superlinear dose dependence of thermoluminescence and optically stimulated luminescence at high dose rates*. Radiat. Meas. **71**, 220–225 (2014).
18. Chen, R., Lawless, J. L. and Pagonis, V. *Thermoluminescence associated with two-electron traps*. Radiat. Meas. **99**, 10–17 (2017).
19. Chen, R., Lawless, J. L. and Pagonis, V. *Thermoluminescence associated with two-hole recombination centers*. Radiat. Meas. **115**, 1–6 (2018).
20. Jain, V. K., Kathuria, S. P. and Ganguly, A. K. *Radiation damage in thermoluminescent  $\text{LiF}$  TLD-phosphor*. J. Phys. C: Sol. St. Phys. **8**, 2191–2197 (1975).
21. Yukihara, E. G., Whitley, V. H., Polf, J. C., Klein, D. M., McKeever, S. W. S., Akselrod, A. E. and Akselrod, M. S. *The effect of deep trap population on the thermoluminescence of  $\text{Al}_2\text{O}_3\text{:C}$* . Radiat. Meas. **37**, 627–638 (2003).
22. Chen, R., Lo, D. and Lawless, J. L. *Non-monotonic dose dependence of thermoluminescence*. Radiat. Prot. Dosimetry **119**, 33–36 (2006).
23. Pagonis, V., Chen, R. and Lawless, J. L. *Non-monotonic dose dependence of OSL intensity due to competition during irradiation and readout*. Radiat. Meas. **41**, 903–906 (2006).
24. Yukihara, E. G., Whitley, V. H., McKeever, S. W. S., Akselrod, A. E. and Akselrod, M. S. *Effect of high-dose radiation on the optically stimulated luminescence of  $\text{Al}_2\text{O}_3\text{:C}$* . Radiat. Meas. **38**, 317–333 (2003).

25. Facey, R. A. *Heating-rate effects in glow peak measurements for thermoluminescence dosimetry*. Health Phys. **12**, 717–720 (1966).
26. Groom, P. J., Durrani, S. A., Khazal, K. A. and McKeever, S. W. S. *The dose-rate dependence of thermoluminescence and sensitivity in quartz*. Europ. PACT J. **2**, 200–210 (1978).
27. Hsu, P. C. and Weng, P. S. *Reaffirmation on the low exposure rate dependence of the CaSO<sub>4</sub>:Dy thermoluminescence dosimeter*. Nucl. Instrum. Meth. **174**, 73–76 (1980).
28. Shlukov, A. I., Shakhovetz, A. I. and Lyasenko, M. G. *A criticism of standard TL dating technology*. Nucl. Instrum. Meth. Phys. Res. Sect B **73**, 373–381 (1993).
29. Valladas, G. and Ferreira, J. *On the dose-rate dependence of the thermoluminescence response of quartz*. Nucl. Instrum. Meth. **175**, 216–218 (1980).
30. Chen, R. and Leung, P. L. *A model for dose-rate dependence of thermoluminescence intensity*. J. Phys. D: Appl. Phys. **33**, 846–850 (2000).
31. Fleming, S. J. *The pre-dose technique: a new thermoluminescent dating technique*. Archaeometry **15**, 13–30 (1973).
32. Aitken, M. J. *Physics and Archaeology*. (Oxford, UK: Clarendon Press) (1974).
33. Zimmerman, J. *The radiation-induced increase of the 100°C thermoluminescence sensitivity of fired quartz*. J. Phys. C: Sol. St. Phys. **4**, 3265–3291 (1971).
34. Fleming, S. J. and Thompson, J. *Quartz as a heat-resistant dosimeter*. Health Phys. **18**, 567–568 (1970).
35. Martini, M., Sibilia, E., Spinolo, G. and Vedda, A. *Pre-dose, TSL and AC conductance interrelation in quartz*. Nucl. Tracks **10**, 497–501 (1985).
36. Chen, R. and Leung, P. L. *Processes of sensitization of thermoluminescence in insulators*. J. Phys. D: Appl. Phys. **31**, 2628–2635 (1998).
37. Chen, R. *Saturation of sensitization of the 110°C peak in quartz and its potential application in the pre-dose technique*. Eur. PACT J. **3**, 325–335 (1979).
38. Pagonis, V. and Carty, H. *Simulations of the experimental pre-dose technique for retrospective dosimetry in quartz*. Radiat. Prot. Dosimetry **109**, 225–234 (2004).
39. Pagonis, V., Chen, R. and Kitis, G. *Theoretical modeling of experimental diagnostic procedures employed during predose dosimetry of quartz*. Radiat. Prot. Dosimetry **119**, 111–114 (2006).
40. Bull, C. and Garlick, G. F. J. *The luminescence of diamonds*. Proc. Phys. Soc. London **63**, 1285–1293 (1950).
41. Hoogenstraaten, W. *Electron traps in zinc-sulphide phosphors*. Philips Res. Repts. **33**, 515–693 (1958).
42. Schulman, J. H., Ginther, R. J., Gorbics, S. G., Nash, A. E., West, E. J. and Attix, F. H. *Anomalous fading of CaF<sub>2</sub>:Mn thermoluminescent dosimeters*. Appl. Radiat. Isot. **20**, 523–529 (1969).
43. Kieffer, F., Meyer, C. and Rigaut, J. *Is isothermal deferred luminescence in organic glasses due to electron tunneling?* Chem. Phys. Lett. **11**, 359–361 (1971).
44. Wintle, A. G. *Anomalous fading of thermoluminescence in mineral samples*. Nature **245**, 143–144 (1973).
45. Visocekas, R. *Tunneling radiative recombination in K-feldspar sanidine*. Nucl. Tracks Radiat. Meas. **21**, 175–178 (1993).
46. Visocekas, R. *Monitoring anomalous fading of TL of feldspars by using far-red emission as a gauge*. Radiat. Meas. **32**, 499–504 (2000).
47. Visocekas, R., Ouchene, M. and Gallois, B. *Tunneling afterglow and anomalous fading in dosimetry with CaSO<sub>4</sub>:Dy*. Nucl. Instrum. Methods **214**, 553–555 (1983).
48. Templer, R. H. *The localized transition model of anomalous fading*. Radiat. Prot. Dosimetry **17**, 493–497 (1986).
49. Tyler, S. and McKeever, S. W. S. *Anomalous fading of thermoluminescence in oligoclase*. Nucl. Tracks Radiat. Meas. **14**, 149–156 (1988).
50. Visocekas, R. and Geoffroy, A. *Tunneling afterglows and retrapping in calcite*. Phys. Stat. Sol. **A41**, 499–503 (1977).
51. Mikhailov, A. J. *The possible role of the tunnel effect in post-irradiation reactions in solid organic materials*. Dokl. Phys. Chem. **197**, 223–225 (1971).
52. Chen, R. and Hag-Yahya, A. *A possible new interpretation of the anomalous fading in thermoluminescent materials as normal fading in disguise*. Radiat. Meas. **27**, 205–210 (1997).
53. Chen, R., Leung, P. L. and Stokes, M. J. *Apparent anomalous fading of thermoluminescence associated with competition with radiationless transitions*. Radiat. Meas. **32**, 505–511 (2000).
54. Lax, M. *Cascade capture of electrons in solids*. Phys. Rev. **119**, 1502–1523 (1960).
55. Mott, N. F. and Gurney, R. W. *Electronic processes in ionic crystals*. (Oxford: Clarendon Press) (1953).
56. Zimmerman, D. W., Rhyner, C. R. and Cameron, J. R. *Thermal annealing effects on the thermoluminescence of LiF*. Health Phys. **12**, 525–531 (1966).
57. Blak, A.R. and Watanabe, S. Proc. 4th Int. Conf. Lumin. Dosim. Krakow. 169–189 (1974).
58. Yossian, D., Mahajna, S., Ben-Shahar, B. and Horowitz, Y. S. *Re-investigation of the kinetic trapping parameters of peak 5 in TLD-100 via 'prompt' and 'residual' isothermal decay*. Radiat. Prot. Dosimetry **47**, 129–133 (1993).
59. Taylor, G. C. and Lilley, E. J. *The analysis of thermoluminescence glow peaks in LiF (TLD-100)*. Phys. D: Appl. Phys. **11**, 567–581 (1978).
60. Gorbics, S. G., Attix, F. H. and Pfaff, J. A. *Temperature stability of CaF<sub>2</sub>:Mn and LiF (TLD-100) thermoluminescent dosimeters*. J. Appl. Radiat. **18**, 625–630 (1967).
61. Pohlit, W. *Zur Thermolumineszenz in lithium fluorid*. Biophysik **5**, 341–356 (1969).
62. Fairchild, R. G., Mattern, P. L., Lengweiler, K. and Levy, P. W. *TL of LiF TLD-100 dosimeter crystals*. IEEE Trans. Nucl. Sci. **NS-21**, 366–372 (1974).
63. Bos, A. J. J., Pijters, T. M., Gómez-Ros, J. M. and Delgado, A. *GLOCANIN, an intercomparison of glow curve analysis computer programs, IRI-93-005*. (The Netherlands: Delft University) (1993).
64. Bilski, P., Obyrk, B., Olko, P., Mandowska, E., Mandowski, A. and Kim, J. L. *Characteristics of LiF:Mg, Cu, P thermoluminescence at ultra-high dose range*. Radiat. Meas. **43**, 315–318 (2008).



65. Mandowska, E., Majgier, R. and Mandowski, A. *Spectrally resolved thermoluminescence of pure potassium chloride crystals*. Appl. Radiat. Isot. **129**, 171–179 (2017).
66. Chen, R. and Hag-Yahya, A. *Interpretation of very high activation energies and frequency factors in TL as being due to competition between centers*. Radiat. Prot. Dosimetry **65**, 17–20 (1996).
67. Mandowski, A. *Topology-dependent thermoluminescence kinetics*. Radiat. Prot. Dosimetry **119**, 23–28 (2006).
68. Sharon, M., Pradhananga, R. R. and Sunta, C. M. *The order of kinetics of thermoluminescence of LiCl single crystals*. J. Phys. C: Solid St. Phys. **13**, 3795–3800 (1980).
69. Kathuria, S. K. and Sunta, C. M. *Order of kinetics for thermoluminescence in LiF TLD-100*. J. Phys. D: Appl. Phys. **15**, 497–505 (1982).
70. Kitis, G., Polymeris, G. S., Sfampa, I. K., Prokic, M., Meriç, N. and Pagonis, V. *Prompt isothermal decay of thermoluminescence in MgB<sub>4</sub>O<sub>7</sub>:Dy, Na and LiB<sub>4</sub>O<sub>7</sub>:Cu,In, in dosimeters*. Radiat. Meas. **84**, 15–25 (2016).
71. Chen, R. and Pagonis, V. *Study of the stability of the TL and OSL signals*. Radiat. Meas. **81**, 192–197 (2015).
72. Chen, R. and Pagonis, V. *A Monte-Carlo study of the fading of TL and OSL signals in the presence of deep-level competitors*. Radiat. Meas. **132**, 106257 (2020).
73. Chen, R., Lawless, J. L. and Pagonis, V. *Two-stage thermal stimulation of thermoluminescence*. Radiat. Meas. **47**, 809–813 (2012).
74. Johnson, P. D. and Williams, F. E. *The interpretation of the dependence of luminescent efficiency on activator concentration*. J. Chem. Phys. **21**, 125–139 (1950).
75. Ewles, J. and Lee, N. *Studies on the concept of large activator centers in crystal phosphors*. J. Electrochem. Soc. **100**, 392–398 (1953).
76. Schulman, J. H., Claffy, E. W. and Potter, R. J. *Concentration dependence of quantum efficiency of luminescence in KCl:Ti*. Phys. Rev. **108**, 1398–1401 (1957).
77. Van Uitert, L. G. *Factors influencing the luminescent emission states of the rare earths*. J. Electrochem. Soc. **107**, 803–806 (1960).
78. Medlin, W. L. *Thermoluminescence properties of calcite*. J. Chem. Phys. **30**, 451–458 (1959).
79. Medlin, W. L. *Thermoluminescence in dolomite*. J. Chem. Phys. **34**, 672–677 (1961).
80. Rossiter, M. J., Rees-Evans, D. B., Ellis, S. C. and Griffiths, J. M. *Titanium as a luminescence centre in thermoluminescent lithium fluoride*. J. Phys. D: Appl. Phys. **4**, 1245–1251 (1971).
81. Wachter, W. *New method for the optimization of thermoluminescence sensitivity in LiF:Mg,Ti*. J. Appl. Phys. **53**, 5210–5215 (1982).
82. Lai, L. J., Sheu, H. S., Lin, Y. K., Hsu, Y. C. and Chu, T. C. *Thermoluminescence of ZrO<sub>2</sub> doped with Yb<sub>2</sub>O<sub>3</sub> following excitation with X rays*. J. Appl. Phys. **100**, 103508 (2006).
83. Tajika, Y. and Hashimoto, T. *Correlation of blue thermoluminescence (BTL) properties with some impurities in synthetic quartz*. Radiat. Meas. **41**, 809–812 (2006).
84. Vij, A., Lochab, S. P., Kumar, R. and Singh, N. *Thermoluminescence response and trap parameters of gamma exposed Ce doped SrS nanostructures*. J. Alloys Compd. **490**, L33–L36 (2010).
85. Chen, R., Lawless, J. L. and Pagonis, V. *A model explaining the concentration quenching of thermoluminescence*. Radiat. Meas. **46**, 1380–1384 (2011).
86. Chen, R. and Winer, S. A. A. *Effects of various heating rates on glow curves*. J. Appl. Phys. **41**, 5227–5232 (1970).
87. Chen, R. and Pagonis, V. *A model explaining the anomalous heating-rate effect in thermoluminescence as an inverse thermal quenching based on simultaneous thermal release of electrons and holes*. Radiat. Meas. **106**, 20–25 (2017).
88. Kumar, M., Chourasiya, G., Bhatt, B. C. and Sunta, C. M. *Dependence of peak height of glow curves on heating rate in thermoluminescence*. J. Lumin. **130**, 1216–1220 (2010).
89. Wintle, A. G. *Thermal quenching of thermoluminescence in quartz*. Geophys. J. R. Soc. **41**, 107–113 (1975).
90. Curie, D. *Luminescence in crystals*. (London: Methuen and Co. Ltd.) (1963).
91. Seitz, F. *An interpretation of crystal luminescence*. Trans. Faraday Soc. **35**, 74–85 (1939).
92. Mott, N. F. and Gurney, R. W. *Electronic processes in ionic crystals*. (New York: Dover Pub. Inc.) (1948).
93. Schön, M. *Zum Leuchtmechanismus der Kristallophosphore*. Z. Phys. **119**, 463–471 (1942).
94. Klasens, H. A. *Transfer of energy between centres in zinc sulphide phosphors*. Nature **158**, 306–307 (1946).
95. Lawless, J. L., Chen, R. and Pagonis, V. *On the theoretical basis for the duplicitous thermoluminescence peak*. J. Phys. D: Appl. Phys. **42**, 155409 (2009).
96. Nanjundaswamy, R., Lepper, K. and McKeever, S. W. S. *Thermal quenching in natural quartz*. Radiat. Prot. Dosimetry **100**, 305–308 (2002).
97. Rasheedy, M. S. and Zahran, E. M. *The effect of the heating rate on the characteristics of some experimental thermoluminescence glow curves*. Phys. Scr. **73**, 98–102 (2006).
98. Subedi, B., Kitis, G. and Pagonis, V. *Simulation of the influence of thermal quenching on thermoluminescence glow peaks*. Phys. Stat. Sol. **A207**, 1216–1226 (2010).
99. Kalita, J. M. and Wary, G. *Effect of thermoluminescence parameters of biotite mineral due to thermal quenching*. J. Lumin. **132**, 2952–2956 (2012).
100. Kitis, G., Polymeris, G. S., Pagonis, V. and Tsiligranis, N. C. *Thermoluminescence response and apparent anomalous fading factor of Durango fluorapatite as a function of the heating rate*. Phys. Stat. Sol. **A203**, 3816–3823 (2006).
101. Pradhan, A. S., Lee, J. I., Chung, K. S., Choe, H. S. and Lim, K. S. *TL glow curve shape and response of LiF:Mg, Cu, Si - effect of heating rate*. Radiat. Meas. **43**, 361–364 (2008).
102. Bos, A. J. J., Poolton, N. R. J., Wallinga, J., Bessière, A. and Dorenbos, P. *Energy levels in YPO<sub>4</sub>:Ce<sup>3+</sup>,Sm<sup>3+</sup> studied by thermally and optically stimulated luminescence*. Radiat. Meas. **45**, 343–346 (2010).
103. Delice, S., Bulur, E. and Gasanly, N. M. *Anomalous heating rate dependence of thermoluminescence in Ti<sub>2</sub>GaInS<sub>4</sub> single crystals*. J. Mater. Sci. **48**, 3294–3300 (2014).

104. Benabdesselam, M., Mady, F., Duchez, J. B., Mebrouk, Y. and Girard, S. *The opposite effects of the heating rate on the TSL sensitivity of Ge-doped fiber and TLD-500 dosimeters*. IEEE Trans. Nucl. Sci. **61**, 3485–3490 (2014).
105. Delice, S., Bulur, E. and Gasanly, N. M. *Thermoluminescence in gallium sulfide crystals: an unusual heating rate dependence*. Phil. Mag. **95**, 998–1006 (2015).
106. Lewandowski, A. C. and McKeever, S. W. S. *Generalized description of thermally stimulated processes without quasiequilibrium approximation*. Phys. Rev. **B43**, 8163–8178 (1991).
107. Sunta, C. M., Ayta, W. E. F., Chubaci, S. and Watanabe, A. *A critical look at the kinetic models of thermoluminescence: I. First-order kinetics*. J. Phys. D: Appl. Phys. **34**, 2690–2698 (2001).
108. Bos, A. J. J. *On the energy conversion in thermoluminescence dosimetry materials*. Radiat. Meas. **33**, 737–744 (2001).
109. Abd El-Hafez, A. I., Yasin, M. N. and Sadek, A. M. *GCAFIT-A new tool for glow curve analysis in thermoluminescence nanodosimetry*. Nucl. Instr. Meth. Phys. Res. **A637**, 158–163 (2011).
110. Haering, R. H. and Adams, E. N. *Theory and applications of thermally stimulated currents in photoconductors*. Phys. Rev. **117**, 451–454 (1960).
111. Dussel, G. A. and Bube, R. H. *Theory of thermally stimulated conductivity in a previously photoexcited crystal*. Phys. Rev. **155**, 764–779 (1967).
112. Böhm, M. and Scharmann, A. *First-order kinetics in thermoluminescence and thermally stimulated kinetics*. Phys. Stat. Sol. **A4**, 99–104 (1971).
113. Simmons, J. G. and Taylor, G. W. *High-field isothermal currents and thermally stimulated currents in insulators having discrete trapping levels*. Phys. Rev. **B5**, 1619–1629 (1972).
114. Agersap Larsen, N., Bøtter-Jensen, L. and McKeever, S. W. S. *Thermally stimulated conductivity and thermoluminescence from Al<sub>2</sub>O<sub>3</sub>*. Radiat. Prot. Dosimetry **84**, 87–90 (1999).
115. Opanowicz, A. *Analysis of thermally stimulated luminescence and conductivity without quasi-equilibrium approximation*. J. Phys. D: Appl. Phys. **40**, 4980–4990 (2007).
116. Pagonis, V. and Kitis, G. *Prevalence of first-order kinetics in thermoluminescence materials: an explanation based on multiple competition processes*. Phys. Stat. Sol. **A249**, 1590–1601 (2012).
117. Chen, R. and Pagonis, V. *On the expected order of kinetics in a series of thermoluminescence (TL) and thermally stimulated conductivity (TSC) peaks*. Nucl. Instr. Meth. Phys. Res. **B312**, 60–69 (2013).
118. Benavente, J. F., Gómez-Ros, J. M. and Romero, A. M. *Numerical analysis of the irradiation and heating processes of thermoluminescence materials*. Radiat. Phys. and Chem. **170**, 108671 (2020).